Plasma Protein Adsorption to Zwitterionic Poly (Carboxybetaine Methacrylate) Modified Surfaces: Chain Chemistry and End-Group Effects on Protein Adsorption Kinetics, Adsorbed Amounts and Immunoblots

Sinoj Abraham · Markian S. Bahniuk ·
Larry D. Unsworth

Abstract Protein–surface interactions are crucial to the overall biocompatability of biomaterials, and are thought to be the impetus towards the adverse host responses such as blood coagulation and complement activation. Only a few studies hint at the ultra-low fouling potential of zwitterionic poly(carboxybetaine methacrylate) (PCBMA) grafted surfaces and, of those, very few systematically investigate their non-fouling behavior. In this work, single protein adsorption studies as well as protein adsorption from complex solutions (i.e. human plasma) were used to evaluate the non-fouling potential of PCBMA grafted silica wafers prepared by nitroxide-mediated free radical polymerization. PCBMAs used for surface grafting varied in charge separating spacer groups that influence the overall surface charges, and chain end-groups that influence the overall hydrophilicity, thereby allows a better understanding of these effects towards the protein adsorption for these materials. In situ ellipsometry was used to quantify the adsorbed layer thickness and adsorption kinetics for the adsorption of four proteins from single protein buffer solutions, viz, lysozyme, α-lactalbumin, human serum albumin and fibrinogen. Total amount of protein adsorbed on surfaces differed as a function of surface properties and protein characteristics. Finally, immunoblots results showed that human plasma protein adsorption to these surfaces resulted, primarily, in the adsorption of human serum albumin, with total protein adsorbed amounts being the lowest for PCBMA-3 (TEMPO). It was apparent that surface charge and chain hydrophilicity directly influenced protein adsorption behavior of PCBMA systems and are promising materials for biomedical applications.

S. Abraham · L. D. Unsworth (✉)
Chemical and Materials Engineering Department,
University of Alberta, Edmonton, AB, Canada
e-mail: larry.unsworth@ualberta.ca

S. Abraham · L. D. Unsworth
National Research Council (Canada),
National Institute for Nanotechnology,
Edmonton, AB, Canada

M. S. Bahniuk · L. D. Unsworth
Biomedical Engineering Department,
University of Alberta, Edmonton, AB, Canada

1 Introduction

Protein adsorption is considered the impetus behind the initiation of multiple host responses [1]. A complex process, it's driven by various forces that exist between surfaces and proteins in solution. Moreover, adsorbed proteins obfuscate the underlying engineered interface [2]. Thus, surfaces that can inhibit or prevent protein adsorption in order to improve biomaterial hemocompatibility, as well as allow for engineered interfaces to directly interact with tissue, are actively being sought [3–6]. Grafting functional polymers is a common surface modification method that may largely suppress protein adsorption and provide improved hemocompatibility, low toxicity, nonimmunogenicity and high water content [7–13]. However, most systems have limited success in preventing long-term biofilm formation [14], long-term material stability [15] and usually suffer in vivo oxidation [16].

That said, surfaces presenting zwitterionic polymers, such as phosphorylcholine, sulfobetaine and carboxybetaine, may overcome many of these limitations [17–19]. The non-fouling nature of zwitterionic surfaces is postulated to arise from the formation of a strong hydration layer

2 Springer

via ionic solvation, surface charge and hydrogen bonding. These properties are also highly influenced by counteracting forces like ionic strength and dipole moment [20]. The deprotonation of the zwitterionic carboxyl group occurs at high pH and therefore the longer spacer groups can act as a shield against charge neutralization with the positive quaternary amine. Physiochemical properties, thought to dictate protein–surface interactions (i.e. end-group chemistry and polymer film charge), can be tuned for zwitterions by altering the distance between the positive quaternary amine and negative carboxyl group via spacer groups [21–23]. Moreover, the role of end-group chemistry on protein adsorption can be controlled as the terminal chemistry on the nitroxide-mediated free radical polymerization (NMFRP) initiator remains on the chain end during polymerization. To this end, silica wafers grafted with PCBMAs containing zwitterionic charge separating methyl, propyl and pentyl spacer groups with β-phosphonate and TEMPO end-groups were employed as a means of studying the protein adsorption kinetics as well as final adsorbed amounts for single protein solutions of lysozyme (Lys), α-lactalbumin (α-La), fibrinogen (Fbn) and human serum albumin (HSA) as model protein solutions. Lys and α-La were selected as they have similar sizes but different charges and internal stabilities. HSA and α-La have similar charges with different molecular weights. Fbn was also used to understand effect size has on adsorption kinetics. Thus, the effect of surface properties, in concert with the nature of the protein, was evaluated to elucidate protein adsorption mechanisms. Finally, protein adsorption from complex solutions was determined by incubating these surfaces in whole human plasma and total analysis of the adsorbed proteome eluted from these surfaces were evaluated using total protein assays, SDS-PAGE and immunoblotting techniques.

Zwitterionic polycarboxybetaine methacrylate (PCBMA) modified surfaces have been shown to largely suppress protein adsorption while affording functional groups for surface functionalization [20]. Surface properties like charge density, ionic strength, hydrophilicity, etc., of the PCBMAs can be varied by (I) introducing different spacer groups between the zwitterionic charges and (II) altering the chain end-group. Hitherto, no systematic evaluation of the effect of these two components upon protein adsorption, either adsorption from single protein or complex protein solutions, to these surfaces has been reported. Moreover, this is thought to augment our recent report on PCBMA functionalized silica nanoparticles where a systematic assessment of the adsorbed mass of proteins was conducted; focusing on correlating the conformational changes of proteins upon adsorption, electrostatic and hydrophilic effects, as well as states of water structures present on each surfaces upon hydration [24].

Controlled radical polymerization techniques are widely used to graft polymers onto biosurfaces. Recently, NMFRP was utilized for surface grafting PCBMA to silica surfaces and the effect of the chain and end-group chemistry on the resulting surface characteristics were extensively analyzed [25]. In general, it has been shown that NMFRP can yield well-defined polymeric brushes with robust control of molecular weight and polydispersity [26–28] and, unlike atom transfer radical polymerization (ATRP), no potentially cytotoxic catalysts or halide residues are used [25–28]. Alkoxyamine derivatives are the starting initiators for NMFRP and at polymerization conditions their dissociation generates the propagating nitroxy radical [28]. Moreover, these alkoxyamines incorporate a coupling agent for tethering to the surface, a nitroxide group for monomer insertion, and the means of tailoring the chain ends [25]. As hydrophilicity of a surface is known to affect protein adsorption, β-phosphonate and TEMPO end-groups were utilized to alter chain hydrophilicity and subsequent hydration [7, 29].

Herein, we report on six PCBMA surfaces synthesized using NMFRP techniques to have varying spacer and end-group characteristics for the express purpose of understanding their individual effects upon protein adsorbed amounts as well as adsorption kinetics. By altering the spacer groups within the system, it is possible to control surface charge density and chain hydration, whereas altering the end-group chemistry should control overall hydrophilicity. In situ spectroscopic ellipsometry was utilized to determine the adsorption kinetics and total adsorbed amount of four different plasma proteins, viz, Lys, α-La, HSA and Fbn, from their single protein solutions in buffer media. Protein adsorption from complex body fluids is also significant for designing biocompatible devices; therefore we also quantified the protein adsorption nature of these surfaces from human blood plasma using immunoblots.

2 Experimental

2.1 Materials and Methods

Chemicals were used as received, unless noted otherwise. Solvents were purified using standard methods prior to use (Sigma-Aldrich). All synthesis was carried out under pure N_2 using Schlenk techniques. Chicken egg white lysozyme (Lys, pI = 11, 14 kDa), bovine α-lactalbumin (α-La, calcium depleted, Type II, pI = 4.3, 14 kDa), human fibrinogen (Fbn, pI = 5.7, 340 kDa) and human serum albumin (HSA, pI = 4.7, 66 kDa) were purchased from Sigma-Aldrich. Platelet poor human plasma was obtained from Canadian Blood Services Research Division and kept

at −80 °C prior to the use. Blood was collected using research ethics board approved protocols, and all plasma was pooled prior to being distributed from Canadian Blood Services Research Division. Moreover, all donors were considered healthy and drug free prior to donating blood. Disodium phosphate and potassium phosphate were used to prepare phosphate buffer (PB). All dilutions and buffers were prepared with syringe filtered (22 μm) Milli-Q distilled deionized water (Billerica, MA). Carboxybetaine methacrylamide (CBMA) monomers with varying spacer groups were synthesized via the quaternization reaction between *N*-[3-(dimethylamino)propyl] methacrylamide with alkylbromoesters and alkoxyamine initiators with silyl functionality were prepared using *β*-phosphonylated nitroxide radical according to previous reported methods [25, see supporting information]. Commercially available TEMPO radical was also used.

2.1.1 Gel-Permeation Chromatography

Gel-permeation chromatography (GPC) has been used to determine the molecular weight (M_n) and polydispersity index (*I*) of the polymers. The GPC is equipped with Agilent G1311A quaternary pump and G1362A refractive index detector. Dimethyl formamide was used to prepare the polymer solution (0.4 % [w/w]) and 10 μL was injected for each analysis. A PL gel (5 μm) mixed-D type column was used and the flow rate was maintained at 1 mL min^{-1} Calibration was performed with polystyrene standard (Polysciences). The GPC chromatograms were included in the supporting information materials as Figs. S1 and S2.

2.1.2 Thermo Gravimetric Analysis

Thermo gravimetric analysis (TGA) was carried out on a TGA Q50 (TA Instruments, New Castle, USA) following the ASTM D3850-94 standard. The surfaces grafted with initiator and polymer were placed on a calibrated platinum pan and inserted into the machine. A blank test was also performed using a bare silicon wafer possessing same surface area. The grafting density on the surfaces was obtained by heating the samples from 25 to 700 °C under dry nitrogen at a constant heating rate of 10 °C/min. The polymer graft densities on these surfaces were determined using TGA with the following equation:

$$\frac{\left(\frac{W}{100-W}\right)100 \times W_{silica}}{100M \, S_{spec}} \times 10^6$$

where W is the weight loss that occurs between 60 and 700 °C corresponding to the decomposition of the silane molecule predetermined with a blank experiment using the known molecular weight polymer. The molecular weight

(*M*) of the grafted silane, the specific surface area (S_{spec}, m^2 g^{-1}) and the weight loss of substrate determined before grafting (W_{silica}) were also used. The initiator graft density was obtained in the range from 0.95 to 1.1 μmol m^{-2}. TGA plot of thermal decomposition of grafted initiator and polymer was included in the supporting information materials as Fig. S3.

2.1.3 X-Ray Photoelectron Spectroscopy

X-ray photoelectron spectroscopy (XPS) was conducted using an AXIS HIS 165 spectrometer (Kratos Analytical) with a monochromatized Al Kα X-ray source (1486.71 eV). Survey spectra (0–1,100 eV) were taken at constant analyzer pass energy of 160 eV, and all high-resolution spectra were acquired with a pass energy of 20 eV, a step of 0.1 eV and a dwell time of 100 ms. The takeoff angles between the film surface and the photoelectron energy analyzer were 90°. Operating pressure was ∼5 × 10^{-10} Torr in the analysis chamber. The peaks were fit using the CasaXPS application software. Binding energies were "calibrated" so that C1 s peaks were 285 eV. The spectral fitting was done using Specslab software and peak position and peak area are used to evaluate the atomic composition (Table 1) and the representative spectra is included in supporting information material (Fig. S4).

2.1.4 Contact Angle Analysis

The contact angles of polymeric surfaces were measured using First Ten Angstroms (FTA) 2000 multi fluid analyzer by fitting a mathematical expression to the shape of the drop and then calculate the slope of the tangent to the drop at the liquid–solid–vapor interface line. Both advancing and receding contact angles were measured for all surfaces.

2.1.5 In Situ Ellipsometry

In situ ellipsometry (Variable Angle Spectroscopic Ellipsometer, VASE HS-190®, J. A. Woollam Co., NE) was used to characterize tethered initiator, grafted polymer, and protein adsorption over a wavelength range of 300–700 nm and an angle of incidence of 70°. Ellipsometry experiments were performed using a 0.5 mL liquid cell, with data being taken every 4 min for 2 h. Surfaces were mounted in the cell and optical alignment performed to optimize signal. Ellipsometric data was modelled with WVASE-32® analysis software (J.A. Woollam Co., Inc). The Cauchy layer model was used to represent the optical dispersion of the various layers, consisting of silica, PCBMA films and the adsorbed proteins and used to determine the film thickness: see supporting information materials.

Table 1 Surface properties and composition of PCBMA grafted surfaces prepared using phosphonate and TEMPO initiators by nitroxide mediated free radical polymerization

Value	Initiator		Phosphonate			TEMPO		
	Phosphonate	TEMPO	PCBMA1	PCBMA3	PCBMA5	PCBMA1	PCBMA3	PCBMA5
(M_n)	486[b]	390[b]	4500[c]	6100[c]	7050[c]	6400[c]	7200[c]	7900[c]
PDI	–	–	1.4	1.2	1.2	1.3	1.2	1.1
Thickness[a] (nm)^2	1.6 ± 0.2	1.2 ± 0.3	17 ± 2	22 ± 1	28 ± 1	21 ± 1	27 ± 2	29 ± 1
Graft density (μmol/m^2)	2.35 ± 0.03	2.42 ± 0.02	0.9 ± 0.02	1.02 ± 0.03	1.04 ± 0.01	1.12 ± 0.02	1.16 ± 0.03	1.17 ± 0.02
Advancing contact angle (°)	43 ± 2	34 ± 2	79 ± 2	65 ± 2	60 ± 2	89 ± 2	83 ± 2	77 ± 2
Receding contact angle (°)	31 ± 2	22 ± 2	45 ± 2	40 ± 2	29 ± 2	62 ± 2	56 ± 2	48 ± 2
C (%)[d]	55.3 ± 1.1 (54.9)	65.2 ± 1.6 (64.7)	6.3 ± 4.3 (6.)	70.7 ± 2.3 (71.5)	72.4 ± 0.6 (74.1)	70.9 ± 1.4 (72.6)	73.8 ± 1.8 (74.6)	75.4 ± 2.6 (76.1)
N (%)[d]	6.2 ± 0.8 (6.8)	7.6 ± 1.2 (8.4)	10.8 ± 1.5 (.2)	1.7 ± 0.6 (9.7)	9.2 ± 0.6 (10.4)	12.4 ± 2.3 (12.8)	12.9 ± 2.6 (12.5)	11.4 ± 1.1 (11.7)
O (%)[d]	32.7 ± 1.7 (30.8)	27.2 ± 1.3 (26.9)	22.1 ± 2.8 (19.1)	16.9 ± 2.6 (18.3)	17.8 ± 0.8 (15.0)	16.7 ± 3.2 (14.6)	13.3 ± 1.7 (12.9)	13.2 ± 2.1 (12.2)
P (%)[d]	5.8 ± 1.2 (7.5)	Nil	0.8 ± 0.2 (0.6)	0.7 ± 0.4 (0.5)	0.6 ± 0.2 (0.5)	Nil	Nil	Nil
N/P	1.07 ± 0.03	Nil	13.5 ± 0.01	16.7 ± 0.0	15.3 ± 0.01	Nil	Nil	Nil
C/N	8.76 ± 0.05	8.43 ± 0.08	5.79 ± 0.21	6.88 ± 0.	. ± 0.14	5.79 ± 0.24	5.95 ± 0.14	6.67 ± 0.12

Values represent an average ± 1 SD, $n = 3$ unless otherwise mentioned

[a] The film thickness obtained from in situ ellipsometry

[b] Theoretical molecular weights of initiators

[c] GPC molecular weights and PDI of polymers obtained by solution polymerization along with the initiator functionalized surface. Chromatograms shown in supporting information (Figs. S2, S3)

[d] Percentage composition values obtained by XPS. The values given in the parenthesis are the theoretical atomic percentage calculated from the M_n and grafting density

2.2 Plasma Protein Adsorption

PCBMA-modified double sided silica wafers (0.5 cm × 0.5 cm) [25] were incubated in 100 % human plasma, as previously reported [8]. Unlike ellipsometry studies, both surfaces of the silica wafer was in contact with protein solution while incubating. Therefore, double sided oxidized wafers were used for functionalization and both surfaces were taken in account for the total surface area. It was observed that the amount of protein adsorbed to a single PCBMA-silica wafer was insufficient for immunoblot or Total Protein analysis. Thus, four silica wafers for each of the various PCBMA-grafted surfaces (2.0 cm^2) were used, yielding enough proteins to quantify. Briefly, wafers were washed in 100 % ethanol (Fisher Scientific) and incubated overnight at 4 °C, removed from ethanol, rinsed thoroughly with PB for 30 min at room temperature. In order to maximize the concentration of eluted plasma proteins the 4 wafers of each kind were incubated together for the remainder of the adsorption and elution procedure. Wafers were incubated in 300 μL of 100 % human plasma for 3 h at room temperature, then washed three times in excess PB. Adsorbed plasma proteins were eluted off of the wafer surface over 24 h, at room temperature, using a 250 μL solution of 2 % sodium dodecyl sulfate (SDS).

2.3 Total Protein Assay

Protein eluted from the PCBMA surfaces was quantified using Bio-Rad DC Protein Assay Kit (Hercules, CA). Briefly, 5 μL aliquots of each eluted protein sample and each point on the standard curve were processed using the components from the assay kit and analyzed at 740 nm (UV/Vis), in duplicate.

2.4 SDS-PAGE and Immunoblot Techniques

Plasma proteins eluted from the PCBMA surfaces were analyzed and identified using reduced SDS polyacrylamide gel electrophoresis (SDS-PAGE) and immunoblot techniques [8]. All consumables and equipment for SDS-PAGE and immunoblot were purchased from Bio-Rad (Hercules, CA). Briefly, eluted proteins were reduced and denatured by adding 0.5 M β-mercaptoethanol and 2 % SDS (final concentration). The entire volume of each eluted protein solution remaining after the DC assay was used for immunoblot. The sample and sample buffer were heated at 95 °C for 5 min before being run on a 12 % separation gel for ~45 min at 200 V and 400 mA. Proteins were transferred to 0.2 μm Immuno-Blot PVDF membranes (Bio-Rad, Hercules, CA) for 1 h at 100 V and 200 mA. Membranes were cut into strips for immunoblot or colloidal gold staining. Each strip was blocked overnight at room temperature on a rocking plate using 2 mL of 10 % skim milk powder in 0.3 μL/mLTween-20 in 0.15 M Tris buffered saline (TTBS). Antibodies (Supporting Information Materials Table S1) used for the immunoblot analysis were used without further purification, at concentrations of 1:1000. Immunoblots were visualized using 350 μL of stabilized TMB substrate (Promega, Madison, WI) per strip. Colour developing reactions proceeded for 15 min before quenching with 2 mL of water. Gold staining was carried out using Colloidal Gold Total Protein Stain protocols (Bio-Rad, Hercules, CA).

3 Results and Discussion

3.1 PCBMA-Modified Surfaces

Alkoxyamines with a silyl coupling agent and a nitroxide radical enable surface grafting with β-phosphonylated or TEMPO end-groups [25]. NMFRP techniques were employed to facilitate surface polymerization of carboxybetaine methacrylate monomers that differed in spacer groups (i.e. methyl, propyl and pentyl) between the positive quaternary amine and negative carboxyl group (Scheme 1) [25]. When initiator grafting density was determined using previously reported methods [25]. Initiator modified surfaces with phosphonate end groups yielded more thickness with similar graft density than that with TEMPO end-group (Table 1). However, it should be noted that given the fact that these are thin films, the initiator thickness values should be taken as only estimates and illustrate differences that occur with polymerization. XPS results (Table 1) show that atomic compositions of all initiator modified surfaces were as expected, as compared to theoretical values. Of interest is the fact that the advancing and receding contact angles for the β-phosphonate initiators were greater than those measured with TEMPO-modified surfaces. Given the chemistry of these two systems, it was expected that TEMPO surfaces would be more hydrophobic; suggesting that the TEMPO end-groups may minimize their interaction with water by burying within the initiator layer.

PCBMA surface polymerization yielded PCBMA-1, 3 and 5 polymers terminated in either β-phosphonate or TEMPO end-groups (Table 1). Using molecular weights (as determined using solution depletion of monomers during polymerization) coupled with determined graft densities, it was found that XPS atomic concentrations were similar to theoretical values for all polymer modified surfaces (Table 1). Polymerization was confirmed as film thicknesses for all modified surfaces increased ~15 to ~27 nm, as compared to initiator surfaces. However, only a fraction of the initiators were utilized, where average initiator graft density was almost twice that of polymer

Scheme 1 The synthesis scheme of β-phosphonylated nitroxide radical (*Step-1*) and BrTMOS (*Step-2*). The β-phosphonylated alkoxyamine (*Step-3*) and TEMPO-alkoxyamine (*Step-4*) was formed as the result of the addition reaction with corresponding nitroxide radical with BrTMOS. The schematic representation of surface initiated NMFRP of carboxybetaine methacrylamide is shown at the *bottom*
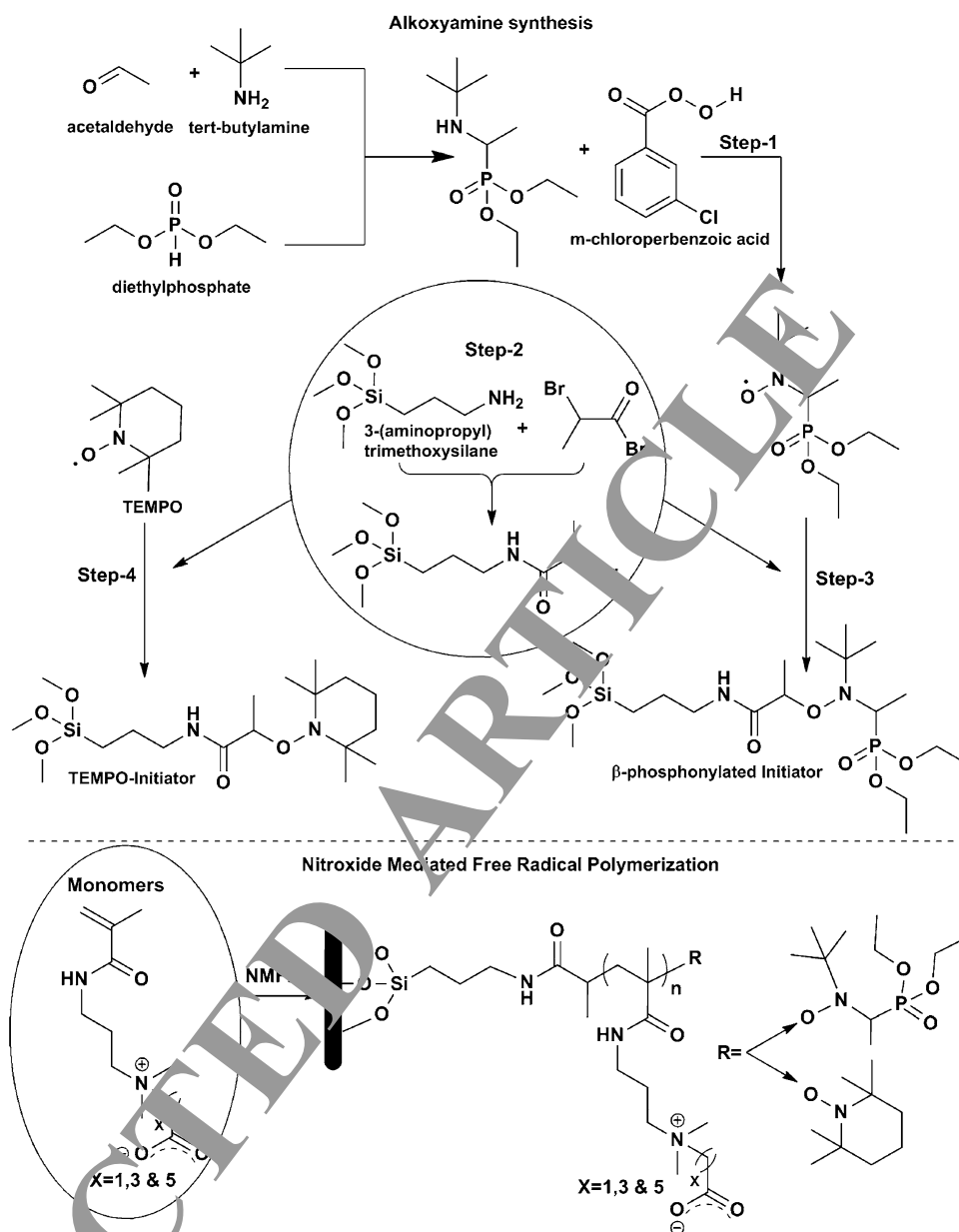
chain graft density. This is commonly observed and usually attributed to a crowding effect that develops during surface initiated polymerization due to the steric hindrance of bulky end-groups and the steric impedance that growing chains impose on near neighboring initiators, which ultimately inhibit their growth [29, 30, 31]. As with the initiator layer, the elemental composition of PCBMA films were similar to expected amounts, illustrating that all PCBMA surfaces formed properly.

End-group chemistry seemed to affect graft density, whereas TEMPO initiators formed films of higher graft density (~1.17 μmol/m²) than β-phosphonate initiators (1.04 μmol/m²) and among them the greatest graft densities were achieved for PCBMA-5 systems. This may be due to the bulky dissociating phosphonate group's presence during

polymerization. PCBMA film thickness seemed to be largely dependant on monomer type, where film thicknesses were PCBMA-5 > PCBMA-3 > PCBMA-1, regardless of end-group. Given the similarity of graft densities for each monomer, within each end-group category, increases in thickness with spacer group may be directly associated with the increase in the polymer M_n (PDI ~ 1) obtained from GPC analysis. The hydrophilic nature of these surfaces was influenced by the initiator and the monomers. Advancing and receding contact angles show that PCBMA-5 (Phospho) surface was the most hydrophilic (adv-60 ± 2° and rec-29 ± 2°) and PCBMA-1(TEMPO) the least (adv-89 ± 2° and rec-62 ± 2°). Interestingly, PCBMA-5 (Phospho) system had a receding contact angle similar to that of the initiator itself, suggesting that the water-polymer brush

interface may be largely populated with phosphonate groups; the same was not observed for any TEMPO system. Contact angles suggest that the hydrophilicity of the surfaces increases with increasing spacer groups. Larger spacer groups provide maximum charge separation, which can result in a higher dipole moment. Chain end-groups also have significant influence on hydrophilicity as these groups are populated as a surface layer of the polymer. TEMPO contains a hydrophobic piperidine ring which should decrease the overall hydrophilic nature of the surfaces. But in aqueous media, this group may also have the tendency to reduce its interaction with water by folding into the polymer layer. These data suggest that TEMPO surfaces exhibit less hydrophilicity than phosphonate surfaces.

3.2 In Vitro Single Protein Adsorption

Single protein solutions of lys, α-La, HSA and Fbn were used to further understand the influence of PCBMA properties on protein adsorption. Spacer groups within the zwitterion of PCBMA can influence charge neutralization on surfaces at relatively high pH [25]. Previous reports detailing the ζ-potentials for systems similar to those presented herein show that polymers with larger spacer groups at high pH conditions (7–10) exhibit a larger variation in charge (24–30 mV) [25] and have the highest pK_a value; which is proportional to spacer length [32]. Showing that the carboxylic acid moieties of PCBMAs remain deprotonated at high pH conditions, but larger spacer groups can potentially minimize the electrostatic coupling. This property of the zwitterionic surface is thought to be crucial for inhibiting protein adsorption [33].

Protein adsorption processes at interfaces are largely characterized by quantifying (i) the adsorption affinity and (ii) the maximum amount adsorbed. Spectroscopic ellipsometry was utilized to study the single protein adsorption trait on PCBMA functionalized silica surfaces using Lys, α-LA, HSA and Fbn as model proteins [4, 35]. Studies were also conducted with bare and initiator grafted silica surfaces as the reference. Lys adsorbed amounts to unmodified surfaces (Fig. 1) was significantly higher ($p < 0.001$, one way ANOVA) than all initiator or polymer modified surfaces. At the saturated state, the surface concentration of Lys on unmodified silica and phosphonate initiator modified surfaces was ∼0.16 and ∼0.107 μg/cm², respectively; values that might be expected for a monolayer, 0.12 μg/cm² [36]. Lys solution concentration didn't significantly alter its adsorption to PCBMA grafted silica wafer surfaces. The effect of the methyl, propyl and pentyl spacer groups on the adsorbed amount of Lys was also examined (Fig. 1b); statistically significance was classified when $p < 0.05$ was obtained using ANOVA analysis. As visible in Fig. 1b, for phosphonate end-groups, PCBMA-5

exhibited the least amount of adsorption (∼0.0018 μg/cm²). As spacer length decreased the amount of adsorbed protein increased, where PCBMA-3 and PCBMA-1 modified surfaces adsorbed ∼0.0035 and ∼0.0039 μg/cm² of Lys. It is thought that as the spacer group within the polymer increased there was greater charge induced repulsion between the surface and the protein. At a pH of 7, Lys is positively charged and previous report on these polymers from our group [24] have shown that surfaces modified with polymers containing larger spacer group have a higher ζ-potential than those with smaller spacer groups. Similar trends in Lys adsorption were observed for PCBMA systems with TEMPO end groups, in that PCBMA-5 (TEMPO) systems adsorbed significantly ($p < 0.001$ in most cases) less Lys compared to polymers with smaller spacer group.

The influence of chain end groups (β-phosphonate and TEMPO) on the reduction of protein adsorption was also studied, where on average, more protein was adsorbed to TEMPO surfaces (Fig. 1b). However, Lys adsorbed amounts were statistically insignificant ($p > 0.05$), except for PCBMA-3 systems where Lys solution concentration was 0.5 and 1 mg/L. The major difference between these two categories seemed to depend on the end-group. β-phosphonate groups offer a bulkier hydrophilic moiety that may regulate the surface hydrophilicity and promote hydrogen bonding with water to form a hydration layer. Another noticeable difference between β-phosphonate and TEMPO surfaces was in surface graft density, and β-phosphonate surfaces exhibit a lower graft density. The hydration of polymeric chains generally decreased with increasing graft chain density [7], but thickly grafted polymer surfaces can effectively resist the proteins with large molecular size [30]. The Lys uptake of PCBMA-5(TEMPO) was 21 % more of that adsorbed on PCBMA-5 (Phospho), while a 8 and 10 % increment was observed for PCBMA-3(TEMPO) and PCBMA-1(TEMPO), respectively. Previously, water hydration studies with PCBMA grafted silica nanoparticles shows that PCBMA-5 can hold the maximum bound water content, potentially providing a means of minimizing protein adsorption to these surfaces [37].

α-La was selected as another model protein for this study because it has a similar size as Lys but opposite charge, providing a mechanism for understanding how the electrostatic properties of PCBMA surfaces may affect protein adsorption. PCBMA surfaces, at a solution pH of 7 or greater, feature a deprotonated carboxylic group that renders a zwitterionic state with the negative carboxylate ion and the positive quaternary ammonium ion. The spacer group greatly defines the overall surface charge at this deprotonated state. As the separation between the oppositely charge ions are lower in small spacer group zwitterionic polymers, the chances for charge neutralization is
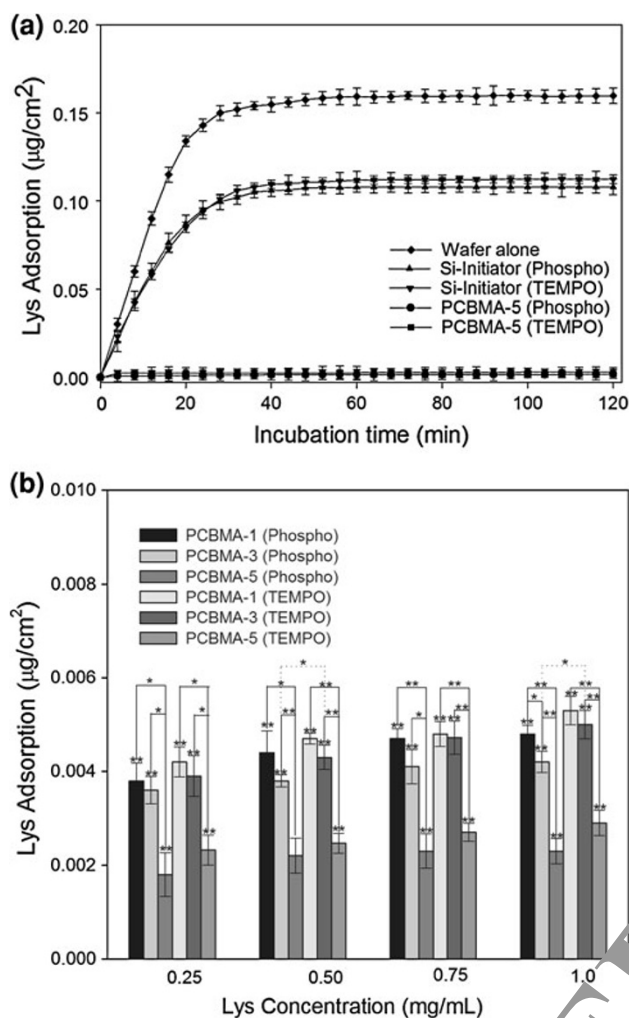
Fig. 1 a Adsorption of lysozyme from PBS buffer (pH 7) for a time period of 2 h. **a** Amount of adsorption *vs.* incubation time on (*filled diamond*) bare oxidized silica wafer (*upward filled triangle*) wafer modified with phosphonate initiator (*downward filled triangle*) wafer modified with TEMPO initiator (*filled circle*) wafer grafted with PCBMA-5 (Phospho) and (*filled square*) wafer grafted with PCBMA-5 (TEMPO). **b** Lys adsorption chart to various PCBMA surfaces at four different concentrations. All these values are statistically significant to silicar wafer grafted corresponding initiators ($p < 0.001$, one way ANOVA). Statistical analysis between surfaces varying spacer and end groups are shown in the figure with *$p < 0.05$ (one way ANOVA), **$p < 0.001$ (one way ANOVA). Data shown represent average $\pm$ 1 SD, $n = 3$
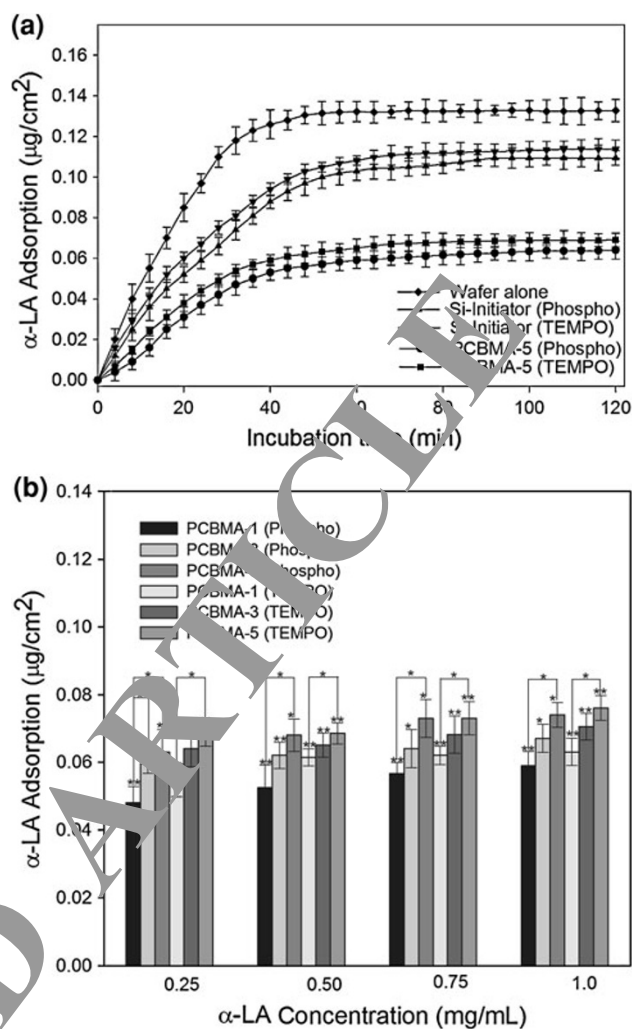
Fig. 2 a Adsorption of β-lactalbumin from PBS buffer (pH 7) for a time period of 2 h. **a** Amount of adsorption versus incubation time on (*filled diamond*) bare oxidized silica wafer (*upward filled triangle*) wafer modified with phosphonate initiator (*downward filled triangle*) wafer modified with TEMPO initiator (*filled circle*) wafer grafted with PCBMA-5 (Phospho) and (*filled square*) wafer grafted with PCBMA-5 (TEMPO). **b** β-la adsorption chart to various PCBMA surfaces and four different concentrations. All these values are statistically significant to silicar wafer grafted corresponding initiators ($p < 0.001$, one way ANOVA). Statistical analysis between surfaces varying spacer and end groups are shown in the figure with *$p < 0.05$ (one way ANOVA), **$p < 0.001$ (one way ANOVA). Data shown represent average $\pm$ 1 SD, $n = 3$

higher compared to the larger spacer group polymers. Therefore, surfaces with larger spacer groups render high surface charge density and therefore they are capable to repel both positive and negative charged proteins to a large extent. Thus, similar to positively charged Lys, the functionalized surfaces also exhibit high resistivity towards the negative α-La (Fig. 2).

The adsorption of α-La to all PCBMA modified surfaces was significantly ($p < 0.001$) lower (~ 0.048–~ 0.07 μg/cm^2) than the reference surfaces (Si- ~ 0.133 μg/cm^2 and

Si/ini- ~ 0.11 μg/cm^2). However, this adsorbed amount of α-La was significantly higher than the amount of Lys adsorbed to these PCBMA systems at similar experimental conditions; being almost ten times greater than Lys adsorption that may arise from the marginally positive nature of PCBMA surfaces [31]. The expected monolayer adsorption of α-La is 0.12–0.15 μg/cm^2 based on its molecular dimensions at the molten globule state on a 0.5 cm^2 surface [38]. The isoelectric point of PCBMA with 1, 3 and 5 spacers were previously reported to be in the

range of pH 8–9 [25]. Therefore negatively charged α-La may interact more strongly with the positive surfaces, resulting in higher protein uptake.

Figure 2b summarizes the adsorption of α-La on surfaces of varying spacer groups and end-groups from different concentrated solutions. The significant influence of spacer groups towards the total amount of α-La adsorbed on PCBMA functionalized surfaces was observed. A reverse trend was observed as that of Lys adsorption, but the values obtained are statistically significant values ($p < 0.05$). PCBMA-1 grafted surfaces exhibited the highest resistance to the adsorption of α-La (~ 0.048 μg/cm^2) compared to PCBMA-3 (~ 0.059 μg/cm^2) and PCBMA-5 (~ 0.063 μg/cm^2). The small spacer groups effectively promote charge delocalization and coupling resulting in a lower surface charge density. Therefore the net positive charge of PCBMA-1 surfaces turns to be less than those grafted with polymers containing a larger spacer group, resulting in lower adsorption of α-La but higher adsorption for Lys. The groups comprising the chain ends also play a significant role as they contribute to enhance the hydrophilicity of surfaces. On average, TEMPO surfaces show a higher adsorption than phosphonate surfaces, but these differences were determined to be insignificant ($p > 0.05$). A similar trend in protein adsorption was observed for phosphonate surfaces, where adsorbed amounts for these surfaces increased with increasing spacer length.

It has been generally considered that the formation of an albumin monolayer at the biomaterial interface is favorable as it may minimize platelet adhesion and activation [39]. Others have indicated that the adsorbed albumin layer, depending on conformation state, may directly affect platelet adhesion and activation [40]. Thus, more specific knowledge regarding HSA adsorption at surfaces is vital for the development of blood-contacting biomaterials. Adsorption studies using HSA were conducted so as to understand the effect protein size has on protein adsorption to these surfaces; where HSA has a similar charge as α-La but is significantly larger. Figure shows a representative profile of protein HSA adsorption and comparative representation of total amount of HSA adsorbed on surfaces of varying spacer and end-groups from solutions of different concentrations. Amount of adsorbed HSA on silica wafers (Si- 0.187 μg/cm^2 and Si/ini- 0.153 μg/cm^2) was significantly higher ($p < 0.05$) than any PCBMA modified surface. HAS's globular nature (dia. ~ 55 Å) needs 0.2 μg/cm^2 to form a closed pack monolayer [41]. At the experimental pH conditions, PCBMA is positively charged and may favor adsorption of negatively charged proteins like HSA. Similar to α-La, HSA adsorption on PCBMA-5 surface (~ 0.029 μg/cm^2) was higher than PCBMA-3 (~ 0.027 μg/cm^2) and PCBMA-1 (~ 0.024 μg/cm^2) surfaces. The total amount of HSA adsorbed on these surfaces

is almost half that of α-La adsorption, illustrating that protein adsorption to these PCBMA surfaces may be strongly influenced by protein size. It may be that the larger amount of adsorbed α-La indicates that this smaller protein may be able to incorporate into the polymer layer itself, whereas the larger HSA cannot, suggesting that the overall polymer film itself may not be fully homogeneous on the length scale of α-La. Larger spacer groups offers maximum charge separation, thereby reducing the probability for charge neutralization. No significant correlations were observed in the test of significance (one way ANOVA, $p > 0.05$) among the adsorbed amounts of HSA on surfaces with varying spacer groups, irrespective of the end-group.

HSA adsorbed mass was higher on surfaces prepared using β-phosphonate initiators as compared to surfaces prepared with TEMPO initiators; being opposite to other proteins. Therefore, end-group chemistry showed significant influence with HSA adsorption while comparing with the adsorption profiles of smaller proteins like Lys and α-La. However, the difference in the total amount of adsorbed HSA between TEMPO and β-phosphonate surfaces was insignificant (one way ANOVA, $p > 0.05$).

Fbn adsorption to modified surfaces was studied to understand the effect of protein size on protein adsorption, as well as indicator of platelet adhesion and activation [39, 42, 43]. Adsorption studies were conducted with bare and initiator grafted silica wafer as references and the respective plateau region corresponding to saturation was observed at 0.23 and 0.16 μg/cm^2, which falls in the range of Fbn monolayer from its molecular dimensions (0.14–0.7 μg/cm^2) [44]. The rate of adsorption of Fbn on PCBMA surfaces are comparatively studied and total amount of Fbn adsorbed on each surfaces are included in Fig. 4.

Fbn has a very high molecular weight, *i.e*, 6-fold greater than HSA, with charge similar to albumins, Fbn adsorption studies provide a platform for understanding the effect of protein size towards adsorption behavior on these surfaces, along with the effect of spacer length and end-group. The longer chain can effectively resist protein adsorption even at a low graft density [45], while shorter chains with high graft density also inhibit adsorption of approaching proteins [46]. All PCBMA modified surfaces exhibit a very low and statistically significant (one way ANOVA, $p < 0.001$) adsorption level when compared to the reference surfaces, and a general trend observed with HSA adsorption with spacer group effect was maintained. Like HSA, Fbn adsorbed amount was half that of α-La. Like α-La (pI = 4.3), fibrinogen exists with a low isoelectric point (pI = 5.7) but very high molecular weight (340 kDa). The PCBMA-1 surfaces exert a less positive charge than those with larger spacer group, therefore like albumins, Fbn adsorption is less with PCBMA-1 surfaces. Few statistically significant relations
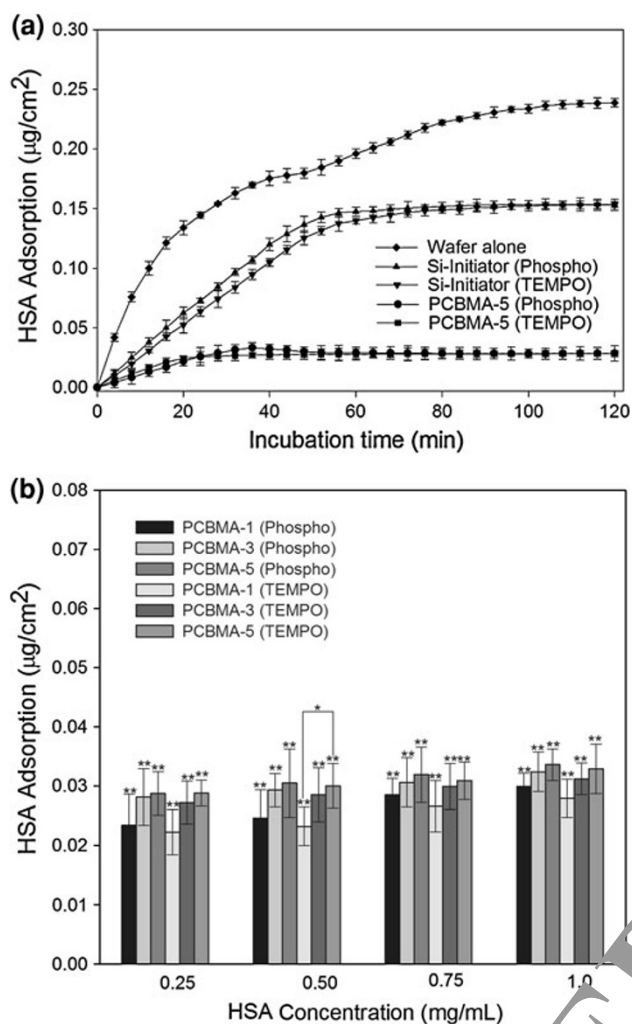
Fig. 3 a Adsorption of HSA from PBS buffer (pH 7) for a time period of 2 h. **a** Amount of adsorption *vs.* incubation time on (*filled diamond*) bare oxidized silica wafer (*upward filled triangle*) wafer modified with phosphonate initiator (*downward filled triangle*) wafer modified with TEMPO initiator (*filled circle*) wafer grafted with PCBMA-5 (Phospho) and (*filled square*) wafer grafted with PCBMA-5 (TEMPO). **b** HSA adsorption chart to various PCBMA surfaces and four different concentrations. All these values are statistically significant to silicar wafer grafted corresponding initiators ($p < 0.001$, one way ANOVA). Statistical analysis between surfaces varying spacer and end groups are shown in the figure with *$p < 0.05$ (one way ANOVA), **$p < 0.001$ (one way ANOVA). Data shown represent average $\pm$ 1 SD, $n = 3$

Fig. 4 a Adsorption of fibrinogen from PBS buffer (pH 7) for a time period of 2 h. **a** Amount of adsorption *vs.* incubation time on (*filled diamond*) bare oxidized silica wafer (*upward filled triangle*) wafer modified with phosphonate initiator (*downward filled triangle*) wafer modified with TEMPO initiator (*filled circle*) wafer grafted with PCBMA-5 (Phospho) and (*filled square*) wafer grafted with PCBMA-5 (TEMPO). **b** Fbn adsorption chart to various PCBMA surfaces and four different concentrations. All these values are statistically significant to silicar wafer grafted corresponding initiators ($p < 0.001$, one way ANOVA). Statistical analysis between surfaces varying spacer and end groups are shown in the figure with *$p < 0.05$ (one way ANOVA), **$p < 0.001$ (one way ANOVA). Data shown represent average $\pm$ 1 SD, $n = 3$

(one way ANOVA, $p < 0.05$) were observed between the β-phosphonate surfaces, varying in spacer length with increase in protein solution concentration. The surfaces with TEMPO terminated chains present a slightly less adsorption that those with β-phosphonate surfaces, but the differences were insignificant. Chain growth on TEMPO initiator surfaces show a greater grafting density with marginally high M_n. Thus, approaching protein may be effectively shielded from the underlying surfaces at this graft density and
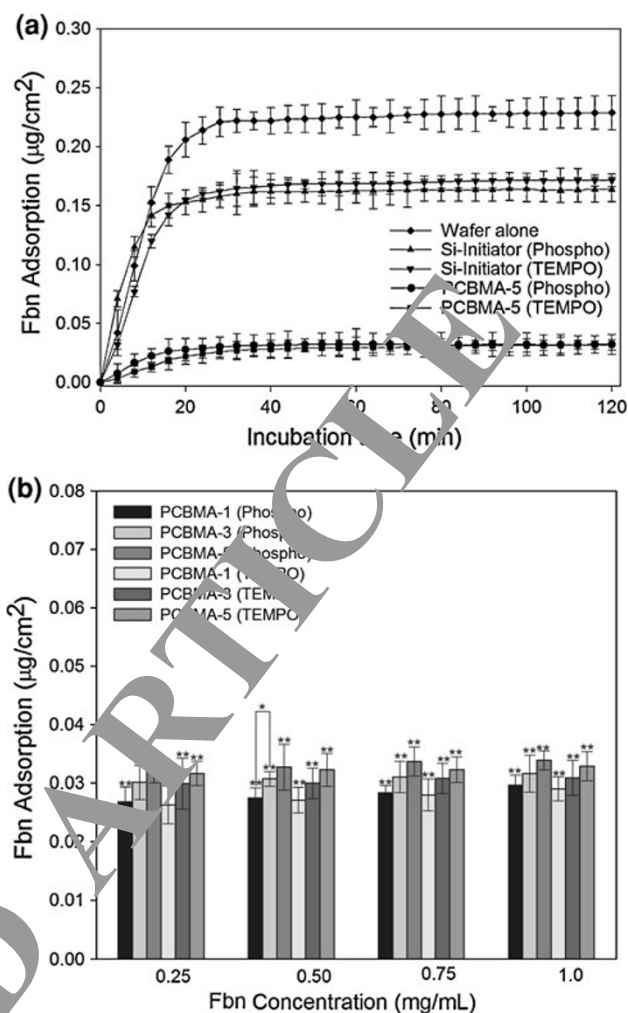
molecular weight, probably due to the increased hydrated steric hindrance associated with the tightly grafted longer PCBMA chains.

Protein adsorption rates were calculated using a non-linear regression analysis of the adsorption model to the experimental data corresponding to adsorption from 0.25 mg/mL concentrated solutions. As there was no statically significant variation in adsorbed amount as a function of protein concentration, 0.25 mg/mL data was chosen for

this analysis (Table 2). The rate of adsorption of proteins is high on blank wafer and decreases upon initiator grafting. Polymer modified surfaces exhibit a 10- to 40-fold lower rate of adsorption than blank wafer. Lys adsorption rate was lower than α-La, even though they have similar molecular size, and HSA was less than α-La, even though they have similar charges; suggesting that adsorption kinetics was not solely diffusion limited. Lys adsorption seems influenced by the spacer and the end-groups of the polymer chain. Adsorption kinetics of α-La and Fbn was higher than that observed with Lys and HSA. This trend obtained with total amount of protein adsorbed with respect to the chain end-groups was also observed for the adsorption kinetics.

Comparing all the single protein adsorption results obtained, there were several similarities. The amount of adsorbed proteins indeed increased sharply within the initial stage of incubation and then slowly proceed as a function of the time until reaching a plateau region in an hour. All surfaces inhibited protein adsorption compared to references. Electrostatic effects between the protein charge and the zwitterionic PCBMA surface is found to be the most significant factor that plays a major role in guiding protein adsorption. At pH 7, PCBMA surfaces are slightly positive charged, so they effectively inhibit the positively charged Lys but promote negatively charged albumins and Fbn to some extent: within the limits of other surface properties like hydrophilicity and graft density. However, among proteins with high pI, the decreased amount of adsorption of HSA and Fbn shows that the size of the protein can be also a deciding factor of overall protein adsorption behavior. High molecular weight proteins are more effectively shielded from PCBMA surfaces and this size effect is observed to be more effective on surfaces that are more thickly grafted, viz, TEMPO surface. Differences in hydrophilic and hydrophobic chain ends were also studied by incorporating corresponding end-groups in relation with their obtained grafting density. These results indicate that rate and amount of protein adsorption on the solid surfaces is highly dependent on the surface properties and the engineered monomers are an easy way to tune surface properties by adjusting various parameters like surface charge, charge density, hydrophility, graft density etc. and provide room for post functionalization.

3.2.1 In Vitro Plasma Protein Adsorption

In this study, plasma protein adsorption was conducted as a means of elucidating any correlations between the properties of the PCBMA surfaces and competitive protein adsorption. Interestingly, a correlation between the total adsorbed amounts from the solution and the results from the model single protein systems seemed to exist; although it's not an easy task to determine the reasons behind the

presence of certain plasma proteins on the surface of biomaterials [47]. While it may be very difficult to conclude the presence of a particular protein as being the product of a particular surface property, the types of proteins present, their qualitative amounts and any potential effects they may have on the surface, other plasma proteins or host responses as a whole are discussed below.

The protein adsorption studies were conducted by incubating surfaces with 100 % platelet poor human plasma for 3 h, and the total adsorbed proteins were eluted off and determined using the Bio-Rad DC assay. This assay can tolerate the presence of up to 10 % SDS. However, the concentration of each protein obtained was lower than the reported effective range of the DC protein assay (0.2–1.5 μg/μL) and well below the sensitivity of any other commercially available protein assay kit. This value indicates that each of the PCBMA surface adsorbs very little protein, despite the relatively high surface area used during the plasma protein adsorption. To identify the proteins eluted from the PCBMA surfaces, SDS-PAGE and Immunoblot techniques were used. The complete list of plasma proteins that are screened for were listed in Table 3. An equal amount of surface area for each sample was used, as were equal times for the colour development reactions so that the differences in band intensities between systems could be compared. The band intensities were quantified using a 13 step grayscale and the results are summarized in Table 3. While comparing the band intensities it is important to understand that different proteins may interact differently with antibodies and, thus, only gross differences in band intensities between different plasma proteins should be considered. Immunoblot techniques can determine the presence or absence of a protein it cannot determine the conformation. It has been shown that a protein's conformation, in addition to its presence or absence, can have an effect on cellular interactions [40].

Colloidal gold staining was used as a general protein stain in order to visualize all protein bands being run on the SDS-PAGE gels. The results of this generalized staining show that there were differences in the absorbed proteome between the various polymer samples. For example, the PCBMA-3 (Phospho) sample showed protein bands at ∼66 and 30 kDa. The results of the immunoblot allow us to identify the 66 kDa band as albumin. The PCBMA-3 (TEMPO) showed a strong protein band at 80 kDa, a tightly packed series of bands ranging from 60–70 kDa as well as sharp bands at 25 and 35 kDa. The immunoblots of this group of eluted proteins did not allow identifying any of these protein bands. These differences in banding suggest that the end-group chemistries play a role in the plasma protein adsorption to PCBMA 3 surfaces. Gold staining of proteins eluted from the PCBMA-5 (Phospho) sample showed species with approximate molecular

Table 2 Adsorption kinetics obtained via non-linear regression analysis of the data corresponding to 0.25 mg/mL protein solution on surfaces with varying spacer and end-groups used for single protein adsorption study

Rate of adsorption ($\times 10^3$ $\mu g/cm^2 min$)	Blank wafer	Initiator		Phosphonate			TEMPO		
		Phosphonate	TEMPO	PCBMA-1	PCBMA-3	PCBMA-5	PCBMA-1	PCBMA-3	PCBMA-5
Lys	6.2 ± 0.4	4.2 ± 0.2	4.5 ± 0.3	0.2 ± 0.1	0.15 ± 0.04	0.04 ± 0.01	0.26 ± 0.12	0.22 ± 0.18	0.1 ± 0.07
α-La	3.5 ± 0.2	2.7 ± 0.1	2.9 ± 0.1	1.5 ± 0.2	1.7 ± 0.1	1.7 ± 0.1	1.6 ± 0.2	1.8 ± 0.1	1.9 ± 0.2
HAS	6.7 ± 0.6	2.9 ± 0.3	2.6 ± 0.5	0.7 ± 0.3	0.9 ± 0.3	0.9 ± 0.2	0.8 ± 0.2	0.9 ± 0.3	1.1 ± 0.4
Fbn	10.9 ± 0.8	6.3 ± 0.4	6.1 ± 0.3	1.3 ± 0.1	1.4 ± 0.1	1.5 ± 0.2	1.1 ± 0.2	2 ± 0.4	1.4 ± 0.3

Table 3 Relative intensities for immunoblots of plasma proteins eluted from the PCBMA systems and amount of plasma proteins eluted from PCBMA-functionalized silica wafers determined using the Bio-Rad DC microplate protein assay

Plasma protein	Fragment size (kDa)	System					
		PCBMA-1 (Phospho)	PCBMA-3 (Phospho)	PCBMA-5 (Phospho)	PCBMA-1 (TEMPO)	PCBMA-3 (TEMPO)	PCBMA-5 (TEMPO)
Albumin	66	*****	*****−	****+	*****	*	****
Alpha1 Antitrypsin	47	****	*	*	*	*	*
Transferrin	77	*****−	*	*	*	*	*
Total eluted protein per surface area ($\mu g/cm^2$)[a]		5.4	3.8	2.9	7.4	6.5	6.3

One star indicates zero band intensity. Five stars indicate a high intensity band. + and − indicate a slightly greater or lesser band intensities respectively

[a] Data represent average of $n = 3$, all have SD of <10 % of the average value. Note that these values are on the lower range of the detection limit of the total protein assay employed, and are shown to illustrate the trend in adsorption

weights of 80, 66, 30 and 25 kDa. Immunoblot identified the strong 66 kDa band to be albumin. This set of binding was also seen for the PCBMA-5 (TEMPO) sample which suggests that the end-group chemistry does not play as important a role in determining plasma protein adsorption.

After being reduced and denatured, albumin runs as a single band with a molecular weight of 66 kDa on an SDS-PAGE gel. This protein was found eluted off of all of the surfaces with the exception of surface grafted with PCBMA-3 (TEMPO). The lack of any detectable albumin in the eluent from PCBMA-3 (TEMPO) is unexpected given its abundance and charge attraction. It may be that this particular polymer has a combination of molecular weight, graft density, hydrophobicity, end-group chemistry and surface charge which work together to prevent HSA adsorption from complex protein solutions. Conversely, there is the possibility that albumin adsorbed in this system is not able to be eluted from the surface. Generally, albumin was present in high amounts as judged by the band intensity. While considering the overall biocompatibility, formation of an albumin monolayer is not considered as harmful as it can inhibit platelet adsorption and activation to some extent, provided they are not overly denatured on

the surface [40]. Though albumin has a negative surface charge like α-La and Fbn, with the exception of PCBMA-3 (TEMPO), the amount of eluted albumin was the same with decrease in as spacer length; unlike the trends observed for single protein adsorption. It is likely that as the surface charge of the PCBMA polymers increases, different and more negatively charged plasma proteins either displace any adsorbed albumin or prevent the albumin from coming into contact with the surface.

α_1-Antitrypsin runs as a single band with molecular weight of 52 kDa, and is considered to an important serine proteases [48]. It was found at a relatively high intensity in the eluent from PCBMA-1(Phospho). At physiological pH levels this protein has a charge of about −12, and thus this high intensity may be due to the opposite charge shown by PCBMA-1 polymers. However, as this protein was not found in the eluent from PCBMA-1(TEMPO) it is clear that the end-group chemistry has some prominent role on the adsorption of this plasma protein, either directly or through its influence on the polymer surface. PCBMA-1(Phospho) has the lowest graft density and molecular weight of any of the tested polymers. This may have some effect on the conformation of the polymer which allows the

adsorption of α_1-antitrypsin from the plasma. This protein is of significance for host response because it is involved in the inhibition of enzymes secreted by neutrophils at the site of inflammation [48].

Transferrin presents as a single band with a molecular weight of about 75 kDa and is primarily responsible for the transport and storage of iron [49]. This protein was found in high amounts, as determined by band intensity, exclusively in the eluent from PCBMA-1 (Phospho). Transferrin does not have a strong charge at pH 7 so its presence on the surface of PCBMA-1 (Phospho) is probably not due to charge interactions. As discussed above for α_1-antitrypsin, the presence of transferrin is most likely due to a combination of other physical characteristics of the polymer.

Plasma proteins that were not found eluted from the PCBMA surfaces can yield just as much information about host response as those which are found. A large number of proteins scanned for do not appear in any sample eluent. For instance, the lack of Factor 1, Complement Factor 3 (C3) or IgG indicates that neither the classical nor alternate pathways of complement were activated by PCBMA surfaces. The absence of IgG is also indicative of a lack of immune response. Nonspecific cell binding to PCBMA surfaces is also unlikely due to the absence of either fibronectin or vitronectin. The lack of plasminogen suggests fibrinolysis does not occur. Activation of coagulation via the contact phase is also not likely due to the absence of high molecular weight kininogen, prekallikrein, Factor XI and Factor XII. These proteins are all involved in activation of coagulation by the extrinsic pathway. Furthermore, the lack of prothrombin, thrombin or fibrinogen further suggests these surfaces do not elicit a pro-coagulant response especially given thrombin's central role in this process [50]. The same can be said for anticoagulant activity as neither protein C nor protein S was found either. The lack of β_2-macroglobulin, a potent inhibitor of both pro and anticoagulant activity, was also observed. These preliminary plasma protein adsorption studies provide a fundamental understanding regarding the hemocompatibility of these designed PCBMA surfaces.

4 Conclusion

In summary, we investigated the efficacy of PCBMA grafted silica surfaces in controlling protein interactions from single and complex protein solutions. Surface properties that influence the protein adsorption were studied by using proteins that varied in size and charge along with surfaces possessing various physiochemical properties. It was demonstrated that the PCBMA surfaces obtained by NMFRP inhibit protein adsorption from human blood plasma. The results obtained in this work suggest that

properties related to surface charge, hydrophilicity and graft density are the main determinants of protein adsorption. Even though, studying the adsorption from single protein or plasma solution are not sufficient for developing materials usable in drug delivery applications or as biomaterials, considering the water solubility and biocompatibility of PCBMA, grafted surfaces such as those reported here offer a new method for preparing surfaces with properties such as a reduced amount of protein adsorption.

References

1. Nakanishi K, Sakiyama T, Imamura K (2001) J Biosci Bioeng 91:233
2. Lynch I, Dawson KA (2008) Nano Today 3:40
3. Brash JL (2000) J Biomater Sci Polym Ed 11:1135
4. Castner DG, Ratner BD (2002) Surf Sci 500:28
5. Service RF (1995) Science 270:230
6. Lee BS, Lee JK, Kim WJ, Jung YH, Sim SJ, Lee J, Choi IS (2007) Biomacromolecules 8:744
7. Unsworth LD, Sheardown H, Brash JL (2008) Langmuir 24:1924
8. Unsworth LD, Sheardown H, Brash JL (2005) Biomaterials 26:5927
9. Unsworth LD, Sheardown H, Brash JL (2005) Langmuir 21:1036
10. Chen H, Brook MA, Sheardown H (2004) Biomaterials 25:2273
11. Alcantar NA, Aydil ES, Israelachvili JN (2000) J Biomed Mater Res Part A 51:343
12. Hayama M, Yamamoto K, Kohori F, Uesaka T, Ueno Y, Sugaya H, Itagaki I, Sakai K (2004) Biomaterials 25:1019
13. Robinson S, Williams PA (2002) Langmuir 18:8743
14. Roosjen A, Van der mei HC, Busscher HJ, Norde W (2004) Langmuir 20:10949
15. Cheng G, Zhang Z, Chen S, Bryers JD, Jiang S (2007) Biomaterials 28:4192
16. Ostuni E, Chapman RG, Holmlin RE, Takayama S, Whitesides GM (2001) Langmuir 17:5605
17. Zhang Z, Chao T, Chen S, Jiang S (2006) Langmuir 22:10072
18. Chapman RG, Ostuni E, Takayama S, Holmlin RE, Yan L, Whitesides GM (2000) J Am Chem Soc 122:8303
19. Ishihara K, Ziats NP, Tierney BP, Nakabayashi N, Anderson JM (1991) J Biomed Mater Res 25:1397
20. Zhang Z, Vaisocherova H, Cheng G, Yang W, Xue H, Jiang S (2008) Biomacromolecules 9:2686
21. Chevalier Y, Leperchec P (1990) J Phys Chem 94:1768
22. Chevalier Y, Storet Y, Pourchet S, Leperchec P (1991) Langmuir 7:848
23. Vaisocherova H, Zhang Z, Yang W, Cao Z, Cheng G, Taylor AD, Piliarik M, Homola J, Jiang S (2009) Biosens Bioelectro 24:1924

24. Abraham S, So A, Unsworth LD (2011) Biomacromolecules 12:3567
25. Abraham S, Unsworth LD (2011) J Polym Sci Part A: Polym Chem 49:1051
26. Parvole J, Laruelle G, Khoukh A, Billon L (2005) Macromol Chem Phys 206:372
27. Oren R, Liang Z, Barnard JS, Warren SC, Wiesner U, Huck WTS (2009) J Am Chem Soc 131:1670
28. Bartholome C, Beyou E, Bourgeat-Lami E, Chaumont P, Zydowicz N (2003) Macromolecules 36:7946
29. Unsworth LD, Tun Z, Sheardown H, Brash JL, Colloid J (2006) Interface Sci 296:520
30. Feng W, Brash JL, Zhu S (2004) J Polym Sci, Part A: Polym Chem 42:2931
31. Bruck A, Mccoy LL, Kilway KV (2000) Org Lett 2:2007
32. Weers JG, Rathman JF, Axe FU, Crichlow CA, Foland LD, Scheuing DR, Wiersema RJ, Zielake AG (1991) Langmuir 7:854
33. Holmlin RE, Chen XX, Chapman RG, Takayama S, Whitesides GM (2001) Langmuir 17:2841
34. Elwing H, Welin S, Askendal A, Lundstrom L, Colloid J (1988) Interface Sci 123:306
35. Thompson DW, Woollam JA (2005) Spectro Intl J 19:147
36. Kim DT, Blanch HW, Radke CJ (2002) Langmuir 18:5841
37. Lide DR (eds) CRC handbook of chemistry and physics, 85th edn. CRC Press, 2004, Chapter 1
38. Gast K, Zirwer D, Muller-Frohne M, Damaschun G (1998) Protein Sci 7:2004
39. Kottke-Marchant K, Anderson JM, Unenura Y, Marchant RE (1989) Biomaterials 10:147
40. Sivaraman B, Latour RA (2010) Biomaterials 31:1036
41. Benesch J, Askendal A, Tengvall P (2000) Colloids Surf B Biointer 18:71
42. Savage B, Ruggeri ZM (1991) J Biol Chem 266:11227
43. Tsai WB, Grunkemeier JM, McFarland CD, Horbett TA (2002) J Biomed Mater Res Part A 60:348
44. Kim J, Somorjai GA (2003) J Am Chem Soc 125:3150
45. Feng W, Brash JL, Zhu S (2006) Biomaterials 27:847
46. Prime KI, Whitesides GM (1993) Am Chem Soc 115:10714
47. Jung SY, Lim SM, Albertorio F, Kim G, Gurau MC, Yan RD, Holden MA, Cremer PS (2003) J Am Chem Soc 125:12782
48. Gettins PGW (2002) Chem Rev 102:4751
49. Moos T, Morgan EH (2000) Cell Mol Neurobiol 20:77
50. Davie EW, Kulman (2006) Semin Thromb Hemost 32:3